Selected static characteristics of a parallel active power filter with feedback from the supply voltage

PIOTR GRUGEL ⊠, JAN MUĆKO

Institute of Electrical Engineering, Bydgoszcz University of Science and Technology
Al. prof. S. Kaliskiego 7, 85-796 Bydgoszcz

e-mail: {⊠ p.gr/mucko}@pbs.edu.pl

Abstract: The article presents selected static characteristics of a parallel active filter with voltage control in the supply line (VPAPF – Voltage-controlled Active Power Filter) as a function of parameters of the supply network. The tests were done on the basis of a simulation model of the supply network and an appropriate compensator. The test results showed that VPAPFs are most suitable for operation in weak networks, maintaining an almost constant level of voltage distortion, regardless of the value of the network impedance. In addition, the influence of the parameter G corresponding to the conductance value suppressing higher harmonics of the network voltage on the operation of the active power filter was determined.

Key words: active power filters, distorted waveforms, harmonic compensation, higher harmonics, mathematical modelling, power quality, voltage deformation

1. Introduction

Active Power Filters (APF) are a well-known tool for suppressing higher harmonics in current and voltage waveforms [1–5]. For practical reasons industry usually uses Parallel Active Power Filters (PAPF), i.e., those in which the converter is connected in parallel to the load. These systems are designed primarily to suppress higher harmonics in the waveforms of current drawn from the network by a non-linear load. In addition, they can compensate for reactive power, as well as the asymmetry of the three-phase energy receiver ("seen" from the network side) [1–4, 6, 7]. However, with traditional control (i.e., one in which the compensating for current waveforms is determined on the basis of identifying the supply current distortions), such filters are not able to compensate for disturbances coming from the powering side [8–13]. The solution to this problem

is to use parallel active power filters also called conductance-controlled filters, whose control is based on the identification of grid voltage distortions at the point of common coupling (PCC) (Voltage-controlled Parallel Active Power Filter, VPAPF), [1, 3, 10–30]. Some publications also use the term "virtual resistance/conductance circuit" [27, 28, 32]. Such controlled active power filters behave like selective conductance [27, 28], the value of which is low for the fundamental harmonic of the supply voltage, and relatively high (equal to the G value) for higher order harmonics. The idea of controlling such a compensator is shown in Fig. 1.
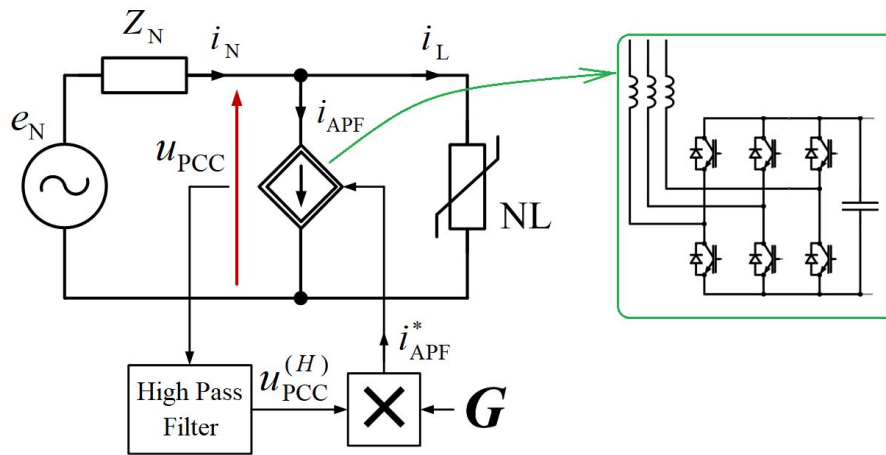

Fig. 1. Conceptual, simplified diagram of a parallel active filter with voltage control in the supply line; e_N – equivalent network voltage (Thevenin voltage), Z_N – equivalent network impedance (Thevenin impedance), NL – nonlinear load

The reference current $i_{APF}^*(t)$ to be introduced by the compensator into the considered node is determined from the following relation:

$$i_{APF}^*(t) = G \cdot u_{PCC}^{(H)}(t), \tag{1}$$

where: $u_{PCC}^{(H)}(t)$ is the harmonic component of the supply voltage waveform at the Point of Common Coupling (PCC), G is the active filter gain (equal to the value of selective conductance). The controlled source shown in Fig. 1 is in fact a power electronic converter controlled in such a way as to introduce a given current waveform i_{APF} to the PCC node.

Figure 2 shows a complete control algorithm for such an active filter. The phase (or interphase) voltage waveforms $u_{PCC\ ABC}$ are transformed into a dq coordinate system rotating with the fundamental harmonic pulsation. Then, the harmonic component of this voltage $u_{PCC\ dq}^{(H)}$ is isolated by the high-pass filter and after multiplying it by the value of the virtual conductance G, a reference current waveform i_{dq}^* is obtained. This current is supplemented with the Δi_d^* component determined by the PI controller in order to stabilize the voltage in the DC bus of the converter (to compensate for losses in the converter). After returning to the static coordinate system $\alpha\beta$, the current regulator (i.e., Dead–Beat) generates the signal waveform of the given voltage $u_{APF\ \alpha\beta}^*$ and then, the SVPWM modulator generates gating signals to switch the power transistors of the converter.

Fig. 2. Schematic diagram of a control algorithm for parallel active filter with voltage control in the supply line; e_N – equivalent network voltage (Thevenin voltage), Z_N – equivalent network impedance (Thevenin impedance), NL – nonlinear load

Thanks to this approach, these filters are effective regardless of whether the source of disturbances is on the load side or on the powering side [10–14]. Moreover, they are capable of suppressing resonance phenomena appearing in the network and preventing their further propagation [11, 15, 17–20, 24, 26–30].

The article presents the static characteristics of the voltage-controlled parallel active filter (VPAPF) as a function of equivalent resistance and equivalent inductance of the power supply network, occurring at selected PCC clamps, and the gain G corresponding to the conductance value of the active filter for the compensated harmonic components. These characteristics were obtained by a computer simulation. For this purpose, an original simulation model of the active power filter and the supply network was developed. Simulation tests were performed using the PSIM simulation software. The control algorithm was implemented in the C++ programming language, and its implementation was made using the DevC++ environment. Using the same environment, the automatic data acquisition and processing of the obtained results were also carried out.

2. Simulation tests

In order to obtain selected static characteristics of the active power filter with conductance control, operating in various conditions, the power supply network was modeled as shown in Fig. 3. The non-linear load (NL), introducing disturbances leading to distortion of supply voltage and current waveforms, consisted of two six-pulse diode rectifiers connected in parallel. The first rectifier was loaded with a 10 Ω resistor shunted 470 μF capacitor. The second rectifier was loaded with a series RL circuit with parameters of 10 Ω and 100 μH and shunted with a capacitor with a capacity of 220 μF. The rectifiers were connected to the PCC through an inductance of 1 μH (which in practice is the inductance of the supply wires). The converter constituting the executive element of the active power filter was modeled as a two-level, transistorized, three-phase bridge with a capacitor in the DC link with a capacity of 820 μF. The converter was coupled to the network via the three-phase L_{APF} choke with an inductance of 200 μH and an internal resistance

of 50 mΩ. The capacitance of the capacitor C_{sh} shunting the active power filter (necessary for such a controlled compensator [16–18, 28]) was 470 μF (in each phase), and taken into account, the capacitor's equivalent series resistance R_{sh} was 5 mΩ. In such a system, the steady-state behavior of the considered active power filter was tested at different values of the network impedance Z_N parameters and at different values of the active power filter gain G.
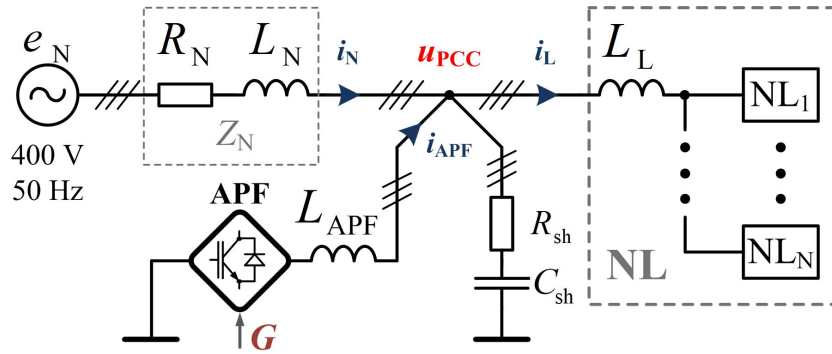

Fig. 3. Diagram of a low-voltage power network with a non-linear load and a voltage-controlled parallel active power filter (VPAPF) used for determining static characteristics

The simulation tests were divided into two parts. In the first part, the equivalent resistance R_N and the equivalent reactance X_N of the network, occurring from the power supply side at the PCC clamps, were changed independently, wherein the reactance value was determined for the fundamental harmonic and from now on it will be understood in this way. The resistance value was changed from 50 mΩ to 1 Ω in 50 mΩ steps, while the reactance value was changed from 0 Ω to 1 Ω with the same steps. As a result, for each determined characteristic, 420 points were obtained. All points were obtained with a constant gain value of $G = 6$. This value was large enough to ensure satisfactory harmonic compensation, and, at the same time, it guaranteed a safe margin of stability. On the basis of the above assumptions, a number of static characteristics was determined, showing the relation between the selected physical quantities occurring at the considered PCC point as a function of resistance and reactance of the supply network. Then, in the second part of the tests, the influence of the gain G value and the equivalent network impedance Z_N on the performance of the considered active power filter was examined. Since the presentation of the characteristics in the function G, R_N and X_N would require the use of four dimensions, the representation of the characteristics was limited to the impedance module $|Z_N|$, assuming equality as to the values of the R_N and X_N parameters. Both quantities were changed from 50 mΩ to 1 Ω in 50 mΩ steps. In turn, the gain value G was changed from 0 to 10 in steps of 0.5. On the basis of the above assumptions, a number of static characteristics were determined, showing the relation between the selected physical quantities occurring in the considered PCC point as a function of the gain G and the value of the impedance module $|Z_N|$.

The value at each point of each obtained characteristic was determined as the arithmetic average of one hundred values calculated from one hundred following periods of the supply voltage waveform in a steady state.

2.1. Obtained static characteristics as a function of equivalent resistance R_N and reactance X_N of the supply network

In order to determine the reference levels needed for further analysis, the characteristics $THD(U_{PCC}) = f(R_N, X_N)$ for the network in Fig. 3, however, operating without a compensator was determined first. The PN-EN 50160 standard provides for the analysis of harmonics up to and including the 40-th order [35]. However, due to the fact, that converter systems can introduce components with much higher frequencies (e.g., carriers), and also due to the phenomena shown later in the article, the calculations were made for a much wider frequency bandwidth. The characteristics made on this basis are shown in Fig. 4.
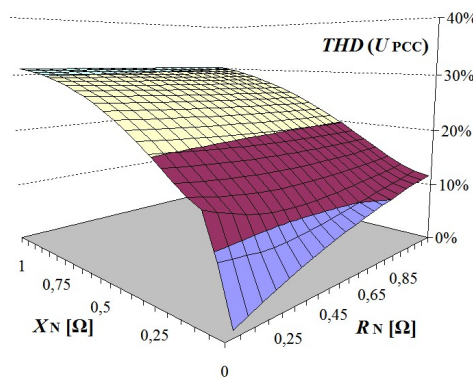
Fig. 4. Static characteristics showing the *THD* of the supply voltage at the PCC point, for various values of equivalent resistance and reactance of the low voltage supply network in the absence of a compensator

With the network impedance close to zero, voltage distortions are small. With the increase in the resistance R_N up to a value of 1 Ω and with the zero-reactance X_N, the harmonic distortion of the supply voltage with the applied load NL increases to 11.9%. With the increase in network reactance up to a value of 1 Ω, the voltage distortion also increases to 31.0%. With a reactance equal to 100 mΩ and a resistance not exceeding 200 mΩ, the fluctuation of the discussed characteristic is noticeable. It is caused by the nature of used non-linear NL load composed of several different non-linear energy receivers, which propagates the greatest disturbances at this network impedance value and in the considered case has a particular influence on increasing the contribution of the 5-th harmonic.

Next, the VPAPF was connected to the PCC node and the tests were repeated. As their result, another characteristic was obtained (Fig. 5). With a low network impedance, the supply voltage distortions are almost non-existent. However, with an increase in the value of this impedance, the voltage *THD* increases slightly. The active filter effectively suppresses unwanted frequency components, keeping the harmonic distortion at a level not exceeding 3.03%. A further increase in both the equivalent resistance and the reactance of the power network does not cause significant changes in the voltage *THD* value, which is a special, and so far, unknown advantage of parallel active filters controlled in this way.
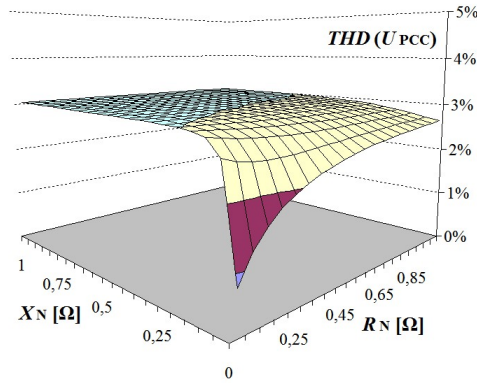
Fig. 5. Static characteristics showing the *THD* of the supply voltage at the PCC point for various values of equivalent resistance and reactance of the low voltage supply network after connecting the compensator

For better visualization of the positive influence of the VPAPF on the power quality and to highlight its role in the modeled network, the distortion attenuation coefficient *k* was introduced. It was defined as the quotient of the voltage *THD* factor at a selected PCC node in the absence of the compensator, to the value of this factor at the same node in the presence of the compensator:

$$k = \frac{THD\,(U_{\text{PCC}})|_{\text{without APF}}}{THD\,(U_{\text{PCC}})|_{\text{with APF}}}. \tag{2}$$

This coefficient carries information about the multiplicity of reducing the distortion of the voltage waveform in the considered PCC node after engaging the VPAPF. The characteristics illustrating the value of the coefficient defined in this way for various network resistance and reactance values are shown in Fig. 6.
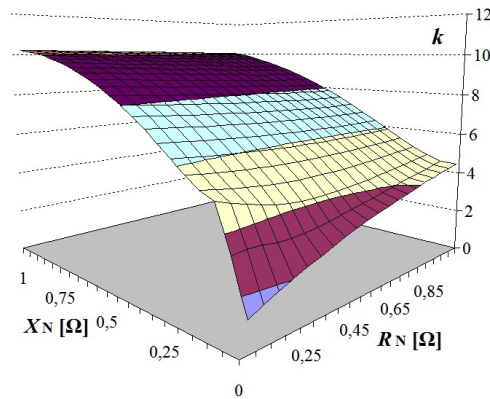
Fig. 6. Static characteristics showing the value of the voltage distortion attenuation coefficient *k* for various values of the equivalent resistance and reactance of the low voltage supply network

For a very low network impedance value (so, practically, with no voltage distortion), the active power filter does not generate significant compensating currents. For this reason, the k-coefficient values are close to unity. With increasing network resistance value (and with zero reactance), the value of the distortion attenuation coefficient increases and at $R_N = 1$ Ω, the k equals 4.50. A similar tendency causes an increase in the network reactance value. With almost zero network resistance and $X_N = 1$ Ω, the voltage waveform shape improves 10.2 times. Alike filtration efficiency occurred at the maximum considered values of network resistance and reactance, where the multiplicity of voltage distortion attenuation was 10.0.

Characteristics $k = f(R_N, X_N)$ show another important advantage of active filters controlled according to the proposed algorithm, namely, their effectiveness increases with the increase in network impedance (so with the increase in susceptibility of this network to voltage distortions, in contrast to conventionally controlled parallel active filters [12, 13]). This relation determines the applicability range of VPAPF systems in very weak power grids.

The characteristics of the current root-mean-square (rms) value introduced by the compensator to the PCC as a function of both components of the network impedance, $I_{APF\ RMS} = f(R_N, X_N)$, were also determined (Fig. 7). For impedance close to zero, the active power filter injects a negligible compensating current due to small distortions of the supply voltage. However, with a slight increase in the X_N value (starting from 50 mΩ), further increase in the resistance value R_N results in the injection of the compensating current I_{APF} into the PCC with an increasingly smaller rms value. This happens e.g., because with the increase in network impedance, due to the increasing voltage drop on this impedance, the value of the supply voltage U_{PCC} decreases, both its fundamental harmonic and the harmonic component $U_{PCC}^{(H)}$. The latter component is the basis for determining the reference compensating current i_{APF}^* (Fig. 1), according to expression (1).
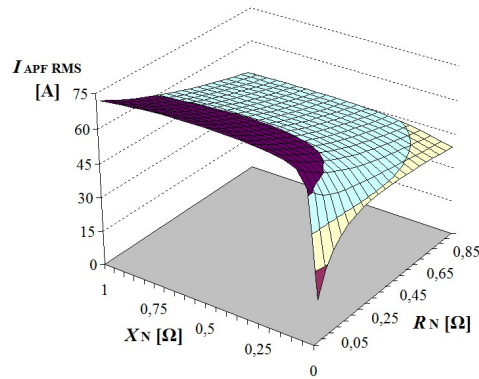

Fig. 7. Static characteristics showing the rms value of the compensating current introduced to the PCC by the active power filter for various values of equivalent resistance and reactance of the low voltage supply network

To designate the utilization level of the compensation current injected by the compensator to the PCC node (in order to improve the shape of the voltage waveform), another auxiliary factor was introduced. It was defined as the quotient of the distortion attenuation coefficient k to the compensating current ($k/I_{APF\ RMS}$), which was injected into the node, causing a k-fold decrease in the voltage deformation in this node. The characteristic (Fig. 8) showing this coefficient informs

about the efficacy of compensation for each ampere of the current I_{APF} injected to the PCC as a function of the supply network resistance and reactance. Apart from inappreciable fluctuations at low values of the network impedance, this characteristic is increasing until the end of the considered range. This means, that with the increase in network impedance, the compensating current I_{APF} introduced to the node by the compensator is used more effectively.
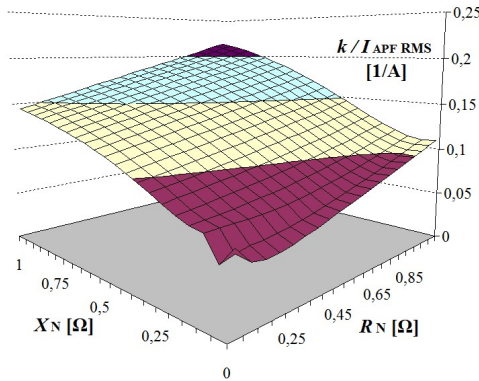

Fig. 8. Static characteristics showing the efficacy level of use of the compensating current for various values of equivalent resistance and reactance of the low voltage power supply network

2.2. Obtained static characteristics as a function of gain G and supply network impedance module $|Z_N|$

Figure 9 shows the characteristic $THD(U_{PCC}) = f(G, |Z_N|)$. For a zero value of gain G, the active power filter does not generate the compensating current I_{APF} (so it is practically an open circuit at its clamps). Increasing the value of G results in a visible suppression of higher harmonics
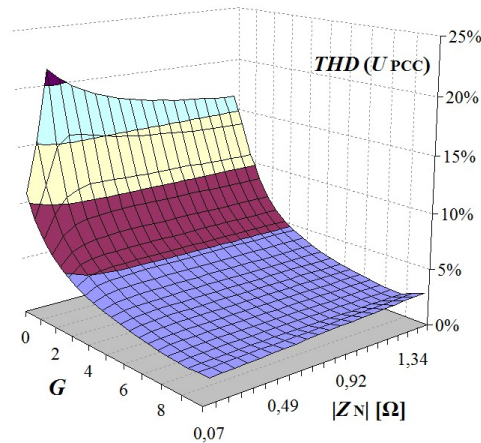
Fig. 9. Static characteristics showing the *THD* of the supply voltage at the PCC node for various values of the gain G and the module of the equivalent impedance of the low-voltage supply network $|Z_N|$

in the supply voltage UPCC, reducing the *THD* to 2 002%. However, after exceeding a value of 8.5 for this parameter, the harmonic distortion starts to increase insignificantly. It is visible in Fig. 8, especially for higher values of the network impedance modulus $|Z_N|$ (over 0.49 Ω). This is because higher gain values bring the system closer to the boundary of the stability margin area. This results in generating oscillations by the active power filter. A further increase in *G* would result in a definite loss of stability of the compensator.

The next characteristic, presented in Fig. 10, illustrates the function of the previously defined distortion attenuation coefficient $k = f(G, |Z_N|)$. An increase in the network impedance module results in an increase in the value of this coefficient. Increasing the gain *G* to the value of 8.5 also increases the value of the *k* coefficient, in this case a 13.4-fold improvement in the supply voltage waveform shape was noted. Further increasing the *G* parameter above a value of 8.5 results in a rapid decrease in the voltage distortion attenuation factor *k* (from 13.4 to 10.0) due to the oscillations introduced by the compensator, which initiate a loss of stability.
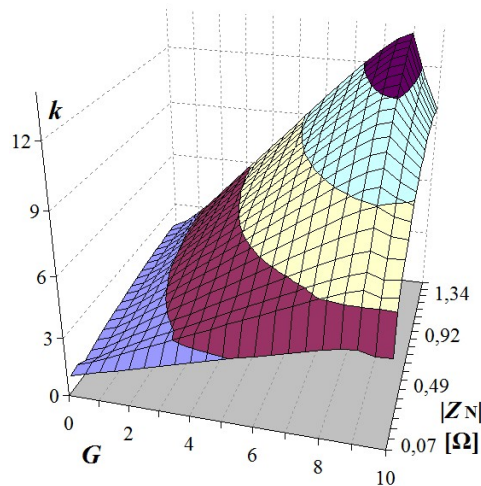

Fig. 10. Static characteristics showing the value of the voltage deformation attenuation coefficient *k* for various values of the gain *G* and the module of the equivalent impedance of the low voltage supply network $|Z_N|$

In the considered system, these oscillations occurred in the band over 2 kHz. This argument supports the legitimacy of conducting the analysis not only in the range of harmonics provided for in the PN-EN 50160 standard [35], but in justified cases in the widest possible band, at least up to the switching frequency of the converter transistors in the power circuit of the compensator [34] (which was done in this study). Therefore, one must be careful not to introduce additional parasitic harmonics when using a filter.

For the considered system, a characteristic showing the rms value of the harmonic component of the supply $U_{\text{PCC}}^{(H)} = f(G, |Z_N|)$ was also determined (Fig. 11). Ideally, this value would be reduced to zero. In practice, it is satisfactory to reduce this component to a value of 8% of the fundamental harmonic for public networks [35], which in the considered case is already at $G = 2$. The noticeable feature of this characteristic is that as the gain increases, the steepness of the characteristic in the direction of the *G* axis (module of derivative $dU_{\text{PCC}}^{(H)}/dG$) decreases. Therefore,

the operation with a too high gain value is not always energetically reasonable. In turn, the increase in the value of $U_{\text{PCC}}^{(H)}$ at $G \geq 8.5$ visible in the characteristics is caused by the oscillations discussed earlier, which are introduced by the VPAPF.
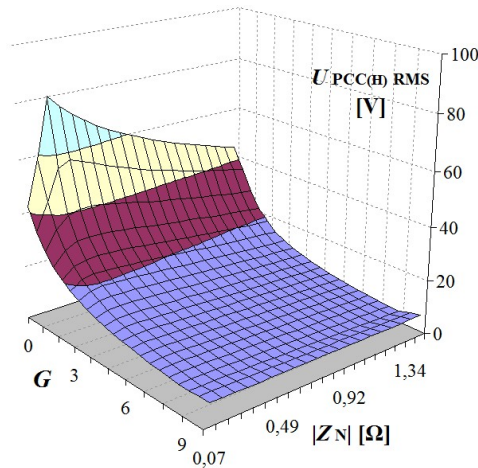

Fig. 11. Static characteristics showing the supply voltage harmonic component rms value for various values of the gain G and the module of the equivalent impedance of the low voltage supply network $|Z_{\text{N}}|$

The characteristic of the rms value of the compensator current $I_{\text{APF RMS}} = f(G, |Z_{\text{N}}|)$ is shown in Fig. 12. It tends to decrease with increasing network impedance. However, as the gain increases, the steepness of this characteristic along the G axis decreases, which means (as in the case above) that operating with too high a gain value is not always reasonable. In addition, an increase in G
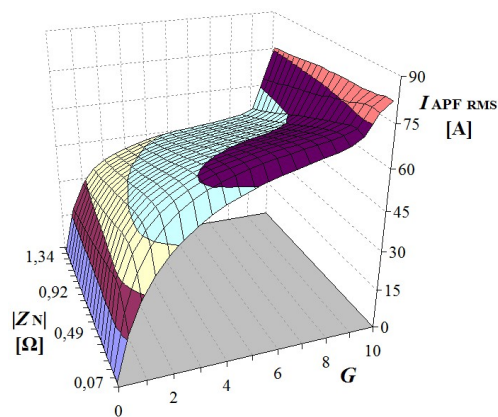

Fig. 12. Static characteristics showing the compensating current rms value introduced to the PCC by active power filter for various values of the gain G and the module of the equivalent impedance of the low voltage supply network $|Z_{\text{N}}|$

above 8.5 results in a rapid increase in the rms value of the compensating current. This is caused by the appearing oscillating component, heralding the risk of stability loss.

The last static characteristic obtained during the tests shows the previously defined compensation current utilization coefficient $k/I_{APF\ RMS}$ (Fig. 13). This characteristic reveals some fluctuations for small values of the network impedance module $|Z_N|$. However, with $|Z_N|$ increase, the value of the compensation current utilization coefficient increases. A similar tendency occurs in the gain function. With increasing G, the characteristic also initially increases, but after exceeding a value of 8.5 there is a very rapid decrease in value due to the appearance of oscillations.
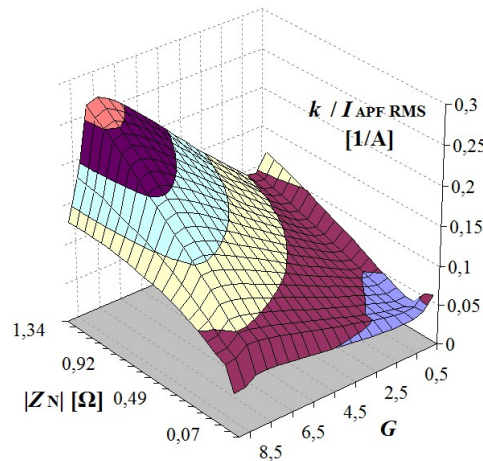
Fig. 13. Static characteristics showing the efficacy level of use of the compensating current for various values of the gain G and the module of the equivalent impedance of the low voltage supply network $|Z_N|$

Thus, too high a gain value results not only in the deterioration of the voltage waveform shape (by introducing an unnecessary oscillating component) but also leads to a very high load (and the risk of overload) of the converter's power circuit.

3. Conclusions

As the research shows, active power filters controlling voltage in the powering line have features that determine the scope of their applicability. One of such features is the fact that VPAPFs are able to maintain an almost constant level of harmonic distortion in the supply voltage, regardless of the equivalent value of the network impedance Z_N, working with a constant value of the gain G (in the conducted research, the gain was 6). This is illustrated by the characteristics in Fig. 5. Additionally, in relatively weak networks (with the value of the equivalent impedance $|Z_N|$ larger than 0.1 Ω), with a further increase of $|Z_N|$, the demand for the rms value of the compensating current, needed to maintain the voltage *THD* at a reduced (constant) value, decreases (Fig. 12 along the $|Z_N|$ axis for $|Z_N| > 0.1$ Ω). Note, that for the value $|Z_N|$ lower than 0.1 Ω, the considered network is relatively strong, so there is practically nothing to compensate. Hence the

small $I_{\text{APF RMS}}$ values in the characteristic area close to the origin of the coordinate system in Fig. 7. The same characteristics show that the tendency of lower demand for compensating current mentioned above is influenced particularly by the network resistance R_{N} (Fig. 7 along the R_{N} axis for X_{N} larger than 0.1 Ω). Moreover, with the increase in the network impedance, the value of the compensation current utilization coefficient $k/I_{\text{APF RMS}}$ increases (Fig. 13). This makes the proposed active filters perfectly suitable for the compensation of higher voltage harmonics in weak networks, and their implementation in such networks allows the use of smaller (cheaper) elements to build a power electronics converter circuit. The gain G, corresponding to the value of conductance shunting unwanted voltage harmonic components in the PCC node, is an essential parameter that allows influencing the intensity of harmonic suppression and the apparent power with which the compensator affects the supply voltage waveforms in the considered node. The relation between gain and filtration effectiveness is not linear (each multiplication of the G value improves the voltage shape by a correspondingly smaller multiplicity), but in most cases it is satisfactory to reduce the level of voltage distortion to 8%, taking into account only 40 first harmonics [35]. Therefore, working with too high gain values is usually unjustified, not only from the energy and economic point of view, but also because of the risk of oscillation and even loss of stability (Fig. 9–13). What is worse, these oscillations may have a higher frequency than the highest harmonic provided for by the standard PN-EN50160 [35] (which was the case in the presented example, Fig. 4, 5), therefore, in the case of using an active power filter, it is reasonable to conduct spectral analysis in a much wider frequency bandwidth [34].

References

[1] Akagi H., Watanabe E.H., Aredas M., *Instantaneous Power Theory and Applications to Power Conditioning*, IEEE Press & Wiley-Interscience A John Wiley & Sons Inc., ISBN: 978-0-470-10761-4 (2007).

[2] Strzelecki R., Supronowicz H., *Harmonic Filtration in AC Power Grids*, Adam Marszalek Publishing House (in Polish), Torun, ISBN: 53-7174-280-0 (1999).

[3] Routimo M., *Developing a Voltage-Source Shunt Active Power Filter for Improving Power Quality*, Tampereen teknillinen yliopisto/Tempere University of Technology, ISBN: 978-952-15-2083-3, E-ISBN: 978-952-15-2117-1, ISSN: 1459-2045 (2008).

[4] Adrikowski T., Buła D., Dębowski K., Maciążek M., Pasko M., *Analysis of selected properties of active power filters*, Silesian University of Technology Publishing House (in Polish), Gliwice, ISBN: 978-83-7335-791-4 (2011).

[5] Zygmanowski M., *Comparative analysis of the properties of selected power electronic converters intended for electrical power conditioning systems*, PhD Thesis (in Polish), Silesian University of Technology, Electrical Department, Gliwice (2009).

[6] Buła D., *Hybrid Active Power Filters*, PhD Thesis (in Polish), Silesian University of Technology, Electrical Department, Institute of Electrical Engineering and Computer Science, Gliwice (2011).

[7] Akagi H., *Modern active filters and traditional passive filters*, Technical Sciences: Bulletin of the Polish Academy of Sciences, vol. 54, iss. 3, ISSN: 0239-7528, e-ISSN: 2300-1917 (2006).

[8] Ozdemir E., Kale M., Ozdemir S., *Active Power Filter for Power Compensation Under Non-Ideal Mains Voltages*, Electric Power Systems Research, vol. 74, iss. 3, ISSN: 0378-7796 (2005).

[9] Ucar M., Ozdemir E., Kale M., *An analysis of three-phase four-wire active power filter for harmonic elimination reactive power compensation and load balancing under nonideal mains voltage*, IEEE 35th

Annual Power Electronics Specialists Conference, PESC 04, ISBN: 0-7803-8399-0, ISSN: 0275-9306 (2004), DOI: 10.1109/PESC.2004.1355329.

[10] Tian H., Li Y.-W., *Output Current Control for Grid Interfacing VSI under Low Switching Frequency and Distorted Grid*, Energy Conversion Congress and Exposition (2015), DOI: 10.1109/ECCE. 2015.7310568.

[11] Grugel P., Strzelecki R., Kłosowski Z., *Comparative analysis of parallel power active filters – typical (current-based) and voltage-based type, working in networks with different topologies*, Przeglad Elektrotechniczny (in Polish), no. 7/2015, ISSN: 0033-2097, E-ISSN: 2449-9544, Sigma Not Publishing House, Warszawa (2015), DOI: 10.15199/48.2015.07.32.

[12] Grugel P., *The influence of the low-voltage network equivalent impedance on the operation of parallel active power filters controlled by two different control algorithms* (in Polish), Przegląd Elektrotechniczny, Sigma Not Publishing House, Warszawa, no. 10/2016, ISSN: 0033-2097, E-ISSN: 2449-9544 (2016), DOI: 10.15199/48.2016.10.47.

[13] Grugel P., Strzelecka N., *The comparative analysis of Parallel Active Power Filters – typical and voltage-based – in various operating conditions*, 9th International Conference on Compatibility and Power Electronics, CPE 2015, ISSN: 2166-9538 (2015), DOI: 10.1109/CPE.2015.7231062.

[14] Grugel P., *Stability analysis of Parallel Active Power Filter operating on the basis of network voltage distortion*, 10th International Conference on Compatibility, Power Electronics and Power Engineering, CPE-POWERENG 2016, e-ISSN: 2166-9546 (2016), DOI: 10.1109/CPE.2016.7544192.

[15] Lee T.L., Li J.C., Cheng P.T., *Discrete Frequency Tuning Active Filter for Power System Harmonics*, IEEE Transactions on Power Electronics, vol. 24, iss. 5, ISSN: 0885-8993 (2009), DOI: 10.1109/TPEL.2009.2013863.

[16] Huan Y.Z., Du Y., *A Novel Shunt Active Power Filter Based on Voltage Detection for Harmonic Voltage Mitigation*, 42nd IAS Annual Meeting of the Industry Applications Conference, ISSN: 0197-2618 (2007), DOI: 10.1109/07IAS.2007.249.

[17] Lee T.L., Cheng P.T., *A Harmonic Damping Method for a Loop Power System*, IAS 2008, ISBN: 978-1-4244-2278-4, E-ISBN: 978-1-4244-2279-1, ISSN: 0197-2618 (2008), DOI: 10.1109/08IAS.2008.269.

[18] Kuo S.-Y., Lee T.-L., Chen Ch.-A., Cheng P.-T., Pan Ch.-T., *Distributed Active Filters for Harmonic Resonance Suppression in Industrial Facilities*, Power Conversion Conference – Nagoya, PCC 2007, ISBN: 1-4244-0843-1, E-ISBN: 1-4244-0844-X (2007), DOI: 10.1109/PCCON.2007.372997.

[19] Lee T.L., Li J.C., Cheng P.T., *A Discrete Frequency Tuning Active Filter for Power System Harmonics*, Power Electronics Specialists Conference, PESC 2008, ISBN: 978-1-4244-1668-4 (2008), DOI: 10.1109/PESC.2008.4591925.

[20] Lee T.-L., Hu S.-H., *Design of Resonant Current Regulation for Discrete Frequency Tuning Active Filter*, The 2010 International Power Electronics Conference, IPEC 2010, ISBN: 978-1-4244-5394-8, E-ISBN: 978-1-4244-5393-1, CD-ISBN: 978-1-4244-5395-5 (2010), DOI: 10.1109/IPEC.2010.5543132.

[21] Ferrari M., *Evaluation of Harmonic Detection Algorithms for Active Power Filter based on Voltage and Current Detection Methods*, 9th IEEE International Symposium on Power Electronics for Distributed Generation Systems, PEDG 2018, ISBN: 978-1-5386-6706-4, E-ISBN: 978-1-5386-6705-7, USB-ISBN: 978-1-5386-6704-0, E-ISSN: 2329-5767 (2018), DOI: 10.1109/PEDG.2018.8447737.

[22] Kumar U., Kumar S., *DC-Link Voltage Balancing with Fuzzy Logic Controller for Shunt Active Power Filter of More Electrical Aircraft*, IEEE First International Conference on Smart Technologies for Power, Energy and Control, STPEC 2020, ISBN: 978-1-7281-8874-4, E-ISBN: 978-1-7281-8873-7, USB-ISBN: 978-1-7281-8872-0 (2020), DOI: 10.1109/STPEC49749.2020.9297762.

[23] Kumar U., Kumar S., *Performance Evaluation of Shunt Active Power Filter for Aircraft System*, International Conference on Electrical and Electronics Engineering, ICE3 2020, ISBN: 978-1-7281-

5847-1, E-ISBN: 978-1-7281-5846-4, USB-ISBN: 978-1-7281-5845-7 (2020), DOI: 10.1109/ICE 348803.2020.9122873.

[24] Akagi H., *Control Strategy and Site Selection of a Shunt Active Filter for Damping of Harmonic propagation in Power Distribution Systems*, IEEE Transactions on Power Delivery, vol. 12, iss. 1, ISSN: 0885-8977, E-ISSN: 1937-4208 (1997), DOI: 10.1109/61.568259.

[25] Szromba A., Mysiński W., *Voltage-source-inverter-based conductance-signal-controlled shunt active power filter*, 19th European Conference on Power Electronics and Applications, EPE 2017 ECCE Europe, ISBN: 978-1-5386-0530-1, E-ISBN: 978-90-75815-27-6, USB-ISBN: 978-90-75815-26-9 (2017), DOI: 10.23919/EPE17ECCEEurope.2017.8099383.

[26] Suryawanshi S., Mahajan S.K., *Reduction of Various Harmonic Resonances in a Power Distribution System by Current Control Method*, 4th International Conference on Inventive Systems and Control, ICISC 2020, ISBN: 978-1-7281-2814-6, E-ISBN: 978-1-7281-2813-9 (2020), DOI: 10.1109/ICISC47916.2020.9171126.

[27] Iturra R.G., Cruse M., Mutze K., Thiemann P., Dresely C., *Power Balance of Shunt Active Power Filter based on Voltage Detection: a Harmonic Power Recycler Device*, IEEE Applied Power Electronics Conference and Exposition, APEC 2019, ISBN: 978-1-5386-8331-6, E-ISBN: 978-1-5386-8330-9, USB-ISBN: 978-1-5386-8329-3 (2019), DOI: 10.1109/APEC.2019.8722037.

[28] Ren B., Wu D., Zhang R., Sun X., Zhang Q., *An Adaptive Droop Control and Virtual Harmonic Resistance Method in Islanding Microgrid*, 13th IEEE Conference on Industrial Electronics and Applications, ICIEA 2018, ISBN: 978-1-5386-3759-3, E-ISBN: 978-1-5386-3758-6, USB-ISBN: 978-1-5386-3757-9, E-ISSN: 2158-2297 (2018), DOI: 10.1109/ICIEA.2018.8398091.

[29] Iturra R.G., Thiemann P., *Comparative Evaluation of Control Strategies for Shunt Active Power Filters in Industrial Power Systems*, PESS + PELSS 2022: Power and Energy Student Summit, ISBN:978-3-8007-6013-8 (2022).

[30] Khan I., Vijay A.S., Doolla S., *Nonlinear Load Harmonic Mitigation Strategies in Microgrids: State of the Art*, IEEE Systems Journal, vol. 16, iss. 3, ISSN: 1932-8184, E-ISSN: 1937-9234, CD-ISSN: 2373-7816 (2022), DOI: 10.1109/JSYST.2021.3130612.

[31] Li Y., He J., Liu Y., *Hybrid APF Background Harmonic Voltage Damping Control Method*, IEEE 9th International Power Electronics and Motion Control Conference, IPEMC 2020 – ECCE 2020 Asia, ISBN: 978-1-7281-5302-5, E-ISBN: 978-1-7281-5301-8 (2020), DOI: 10.1109/IPEMC-ECCEAsia48364.2020.9368244.

[32] Lei Y., Zhao Z., He F., Lu S., Yin L., *An improved virtual resistance damping method for grid-connected inverters with LCL filters*, IEEE Energy Conversion Congress and Exposition, ISBN:978-1-4577-0542-7, E-ISBN:978-1-4577-0541-0, CD-ISBN: 978-1-4577-0540-3, ISSN: 2329-3721, E-ISSN: 2329-3748 (2011), DOI: 10.1109/ECCE.2011.6064287.

[33] Sato Y., Kawase T., Akiyama M., Kataoka T., *A control strategy for general-purpose active filters based on voltage detection*, IEEE Transactions on Industry Applications, vol. 36, iss. 5, ISSN: 0093-9994, E-ISSN: 1939-9367 (2000), DOI: 10.1109/28.871290.

[34] Hoevenaars A., Farbis M., McGraw M., *Active Harmonic Mitigation – What the Manufacturers don't tell you*, IEEE Industry Applications Magazine, vol. 26, iss. 5, ISSN: 1077-2618, E-ISSN: 1558-0598 (2020), DOI: 10.1109/MIAS.2020.2982484.

[35] https://sklep.pkn.pl/pn-en-50160-2010p.html – *PN-EN 50160 – Voltage Characteristics of Public Distribution Systems*, ©Polish Committee for Standardization (in Polish), accessed June 2023.